NANO LETTERS
Letter
Cite This: Nano Lett. XXXX, XXX, XXX−XXX
pubs.acs.org/NanoLett

Phonon Coupling between a Nanomechanical Resonator and a Quantum Fluid

King Yan Fong,*,† Dafei Jin,‡ Menno Poot,†,§ Alexander Bruch,† and Hong X. Tang*,†

†Department of Electrical Engineering, Yale University, New Haven, Connecticut 06511, United States
‡Center for Nanoscale Materials, Argonne National Laboratory, Argonne, Illinois 60439, United States
§Physik-Department, Technische Universitat Munchen, 85747 Garching, Germany

Supporting Information

ABSTRACT: Owing to their extraordinary sensitivity to external forces, nanomechanical systems have become an important tool for studying mesoscopic physics and realizing hybrid quantum systems. While nanomechanics has been widely applied in solid-state systems, its use in liquid receives less attention. There it finds unique applications such as biosensing, rheological sensing, and studying both classical and quantum fluid dynamics in unexplored regimes. In this work, we demonstrate efficient coupling of a nano-optomechanical resonator to a bosonic quantum fluid, superfluid ^{4}He, through ultrahigh-frequency phonons (i.e., sound waves) approaching gigahertz frequencies. A high phonon exchange efficiency >92% and minimum excitation rate of 0.25 phonons per oscillations period, or equivalently $k_B T/hf_m Q_m = 0.044 \ll 1$, are achieved. Based on our experimental results, we further predict that strong coupling between a nanomechanical resonator and superfluid cavity phonons with cooperativity up to 880 can be achieved. Our study opens new opportunities in controlling and manipulating superfluid at the nanoscale and low-excitation level.

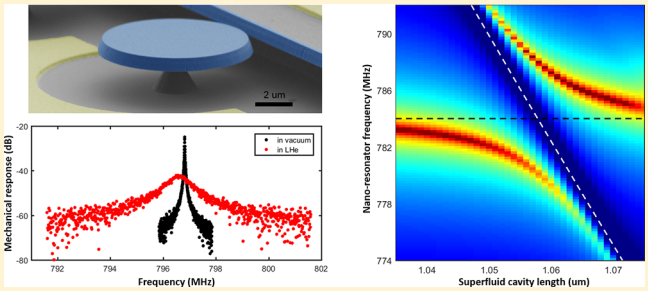

KEYWORDS: *Nanomechanical systems, quantum fluid, superfluid ^{4}He, optomechanics, hybrid quantum systems*

The extreme sensitivity of nanoscale mechanical resonators to external forces allows them to couple to a wide range of physical systems such as photons at optical[1,2] and microwave/radio-frequencies,[3] electron charge[4] and spin,[5] defect centers in solids,[6,7] and superconducting qubits.[8,9] This makes them a versatile tool for studying mesoscopic physics and realizing hybrid quantum systems.[10,11] In addition to the confined resonant vibrations, traveling acoustic phonons also show potential for probing various systems and facilitate long-range communications between on-chip components.[12−15]

To date, while much effort has been made in applying nanomechanics in solid-state systems, fewer works have addressed its use in the fluidic phase, where it enables, for example, studies of fluid dynamics in unexplored regimes,[16−18] as well as biosensing and rheological sensing.[19−24] Of particular interest is its use in superfluid ^{4}He, which itself is a macroscopic quantum object with strong quantum correlation and nonlinearities. While macroscopic mechanical resonators have been used as transducers in superfluid, e.g., vibrating wires,[25] grids,[26] crystal oscillators,[27] tuning forks,[28,29] and more recently MEMS resonators,[30,31] their relatively large size and low oscillation frequency, however, limit their use to probing the average thermodynamic properties of the superfluid at macroscopic scales only. In this respect, nanomechanical systems offer new opportunities for studying superfluid dynamics in low-excitation level down to the quantum limit and at length scales comparable to, or even below, the superfluid coherence length.[32] Attempts of operating nanobeam resonators in liquid helium were made, but the low quality-factor $Q \approx 10$ even in the superfluidic phase hinders their usage as high quality transducers.[32,33] Recently, there has been a rising interest in utilizing superfluid ^{4}He in optomechanical systems[34−37] to take advantage of its low-loss property as a mechanical resonator. To date, those systems, however, suffer from a low optomechanical coupling rate which undermines the efficiency of optomechanical cooling and control.

Here in this work we demonstrate efficient coupling of a nanomechanical resonator to phonons in superfluid ^{4}He. By operating a nano-optomechanical microdisk resonator at ultrahigh frequencies in superfluid ^{4}He, we show that the resonator dynamics are predominately determined by the phonon coupling to the superfluid; i.e., first-sound waves in superfluid are excited causing radiation damping and loading. High quality-factors of $Q \approx 850$ in liquid are demonstrated. Our device achieves high phonon exchange efficiency over 92%

Received: February 25, 2019
Revised: April 25, 2019
Published: April 30, 2019

DOI: 10.1021/acs.nanolett.9b00821
Nano Lett. XXXX, XXX, XXX−XXX

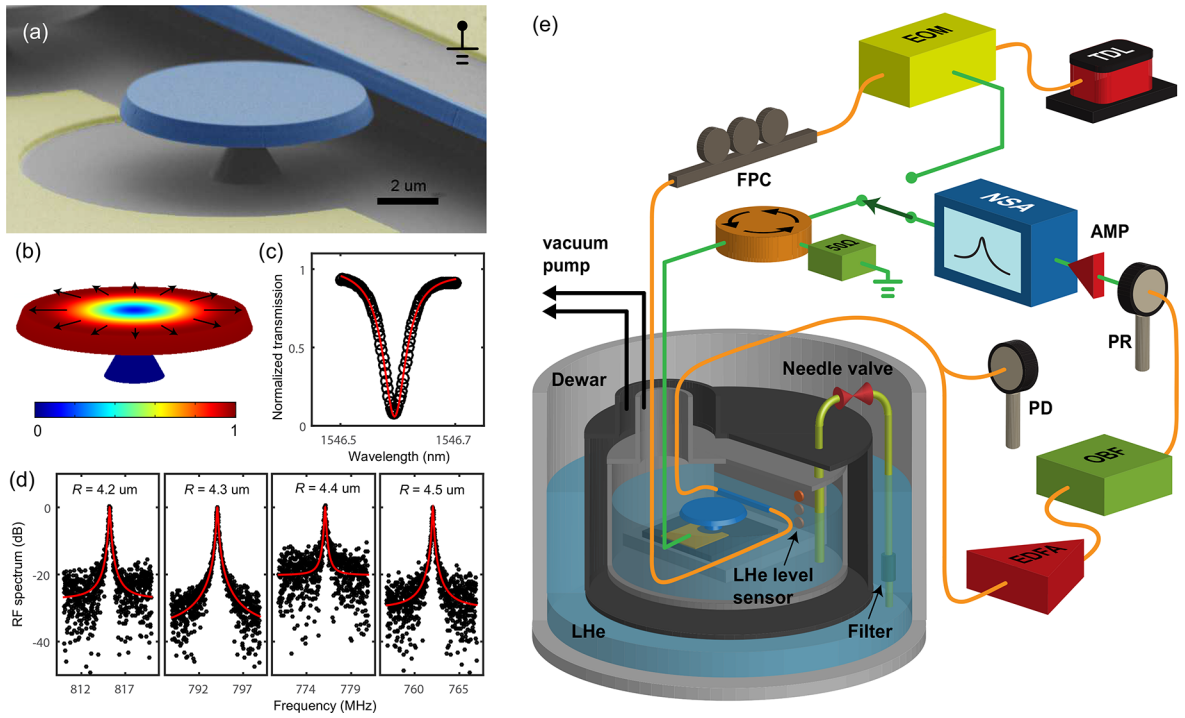

Figure 1. Device and measurement setup. (a) SEM image of a fabricated device with false color. The microdisk and waveguide are shaded in blue, and the electrodes are shaded in yellow. (b) Normalized displacement profile of the fundamental radial breathing mode simulated using FEM. The arrows show the direction of the displacement. (c) Spectrum of a measured optical resonance showing an optical quality factor of 30 000. (d) Normalized RF response of the radial breathing mode of the microdisks measured in vacuum at room temperature. (e) Schematic of the measurement setup. TDL: Tunable Diode laser. EOM: Electro-optic phase modulator. FPC: Fiber polarization controller. PD: Photodetector. EDFA: Erbium-doped fiber amplifier. OBF: Optical bandpass filter. PR: High-speed photoreceiver. AMP: Electrical amplifier. NSA: Network/spectrum analyzer.

and a low excitation level of 0.25 phonons per oscillations period. The latter is equivalent to $k_B T/hf_m Q_m = 0.044 \ll 1$, showing promising potential for operation in the quantum regime. To the best of our knowledge, this value is the lowest among all demonstrations of micro-/nanomechanical resonators immersed in superfluid Helium. Moreover, we show that strong coupling with a cooperativity up to 880 between the nanomechanical resonator and superfluid cavity phonons is within reach. This provides new opportunities to control and manipulate superfluid at the nanoscale with low-level excitations. The low loss superfluid phonons also facilitate long-life quantum information storage and long-range quantum acoustic communication.

The device under study is a nano-optomechanical microdisk resonator made of piezoelectric AlN.[38,39] A scanning-electron micrograph of a fabricated device is shown in Figure 1a. Its mechanical radial breathing mode is coupled to the low-loss optical whispering gallery mode, which efficiently transduces the mechanical displacement into optical signals. The normalized displacement profile of the fundamental radial breathing mode simulated by a finite-element method (FEM) is shown in Figure 1b. Figure 1c shows a typical measured optical resonance, which has an optical quality factor of around 30 000. The device can be driven piezoelectrically by applying radio frequency signals to the electrode fabricated in close proximity to the microdisk. A series of microdisks with top radii of R = 4.2, 4.3, 4.4, 4.5 μm are studied. The measured spectra of their fundamental radial breathing modes are shown in Figure 1d.

The experimental setup is illustrated in Figure 1e. The device performance was first measured in vacuum. At room temperature (T = 295 K), the measured resonance frequencies of the four microdisks are f_m = 815.2, 794.0, 776.0, and 761.9 MHz, which follow the expected $1/R$ dependence (see Supporting Information). The mechanical quality factor Q_m and fractional shift of resonance frequency $\Delta f/f_m$ are plotted versus temperature in Figure 2a and 2b. As the temperature is lowered, the frequencies increase and reach a maximum at around 9 K before receding back slightly. The quality factors show a more dramatic increase from around 4400 at room temperature to 170 000 at 1.45 K. Below 9 K a T^{-1} dependence of Q_m can be observed, while above 9 K the Q_m roughly follows $T^{-1/2}$ with a broad hump appearing at T = 30−200 K. We remark that mechanisms such as the Akhieser effect and thermoelastic effect could lead to $Q_m \approx T^{-1}$[40] and the presence of structural defect states could give rise to nonmonotonic T dependence of Q_m in the mid-temperature range;[41] however, further investigation is needed to confirm the origin of the observed dissipations.

When the device is immersed in liquid ^{4}He, both the resonance frequency and quality factor are reduced as shown in Figure 2c. At T = 4.2 K, Q_m has dropped by almost a factor of 60, to about 1000. On the other hand, f_m only shows a minute down-shift of 0.03%. Figure 2d and 2e plot the frequency response, the peak displacement, and the quality factor at varying driving power measured at T = 1.45 K. Actual displacement is calibrated using the phase modulation method.[42] The result shows that the displacement remains linear to the drive and that the quality factor stays constant up

DOI: 10.1021/acs.nanolett.9b00821
Nano Lett. XXXX, XXX, XXX−XXX

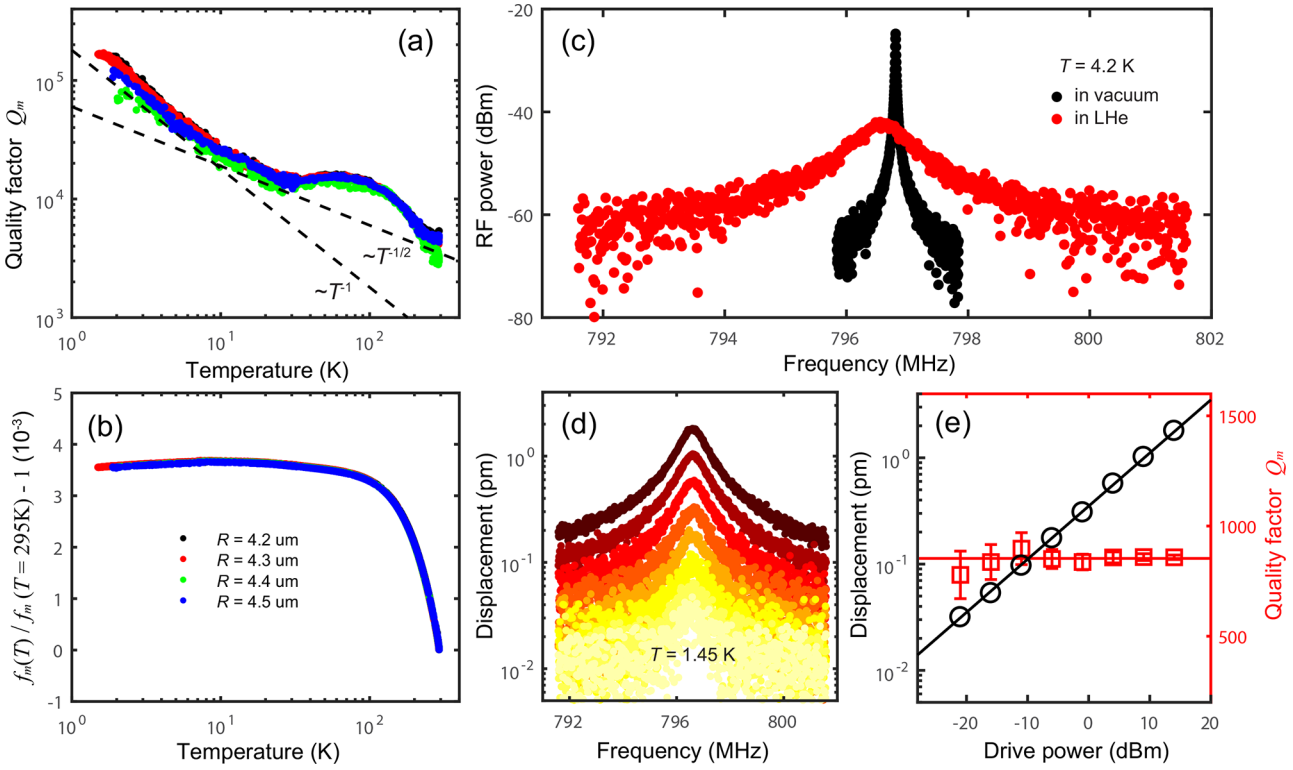

Figure 2. Device characteristics in vacuum and in liquid ^{4}He. (a) Mechanical quality factor Q_m measured in vacuum plotted against temperature. The black dashed lines show the trends of T^{-1} and $T^{-1/2}$. (b) Relative frequency shift $f_m(T)/f_m(T = 295\ \mathrm{K}) - 1$ measured in vacuum plotted against temperature. (c) Mechanical resonances measured in vacuum and in liquid ^{4}He at $T = 4.2$ K for the device with $R = 4.3$ μm. (d) Mechanical response measured at varying driving power. (e) The peak displacement and quality factor measured at varying driving power. The largest displacement attained is 1.78 pm.

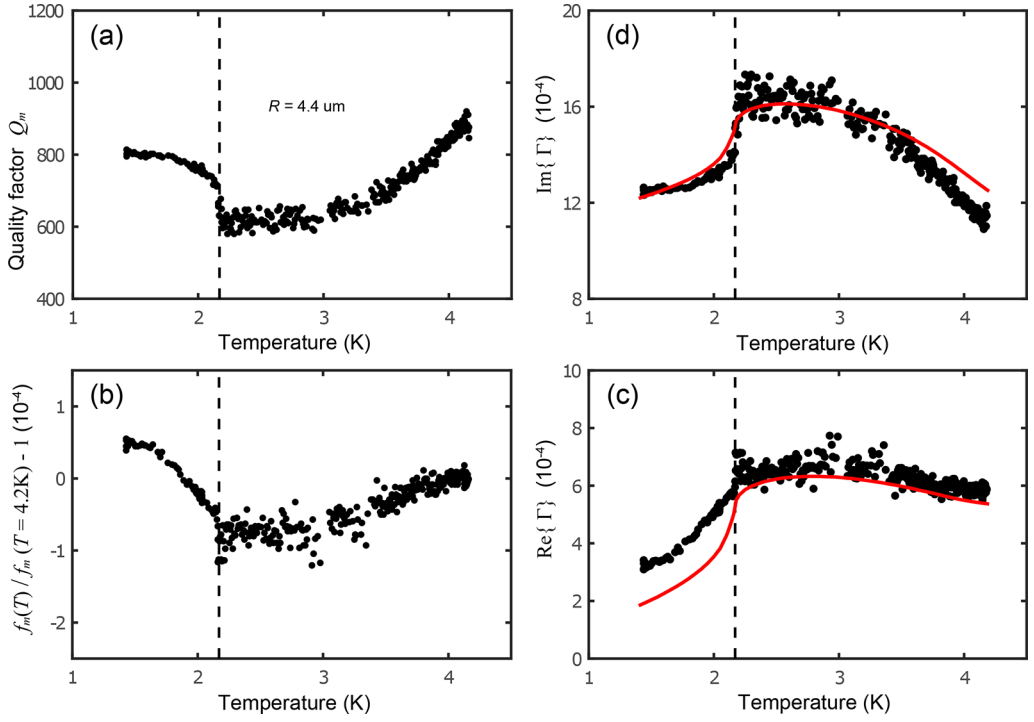

Figure 3. Device characteristics measured in liquid ^{4}He compared with theory. (a) Mechanical quality-factor Q_m and (b) relative frequency shift $f_m(T)/f_m(T = 4.2\ \mathrm{K}) - 1$ plotted against temperature. The black dashed line indicates the λ-point $T = 2.17$ K. (c) Real part Re{Γ} and (d) imaginary part Im{Γ} of the hydrodynamic function plotted versus temperature. The red solid lines represent the numerical result based on the theoretical model.

DOI: 10.1021/acs.nanolett.9b00821
Nano Lett. XXXX, XXX, XXX−XXX

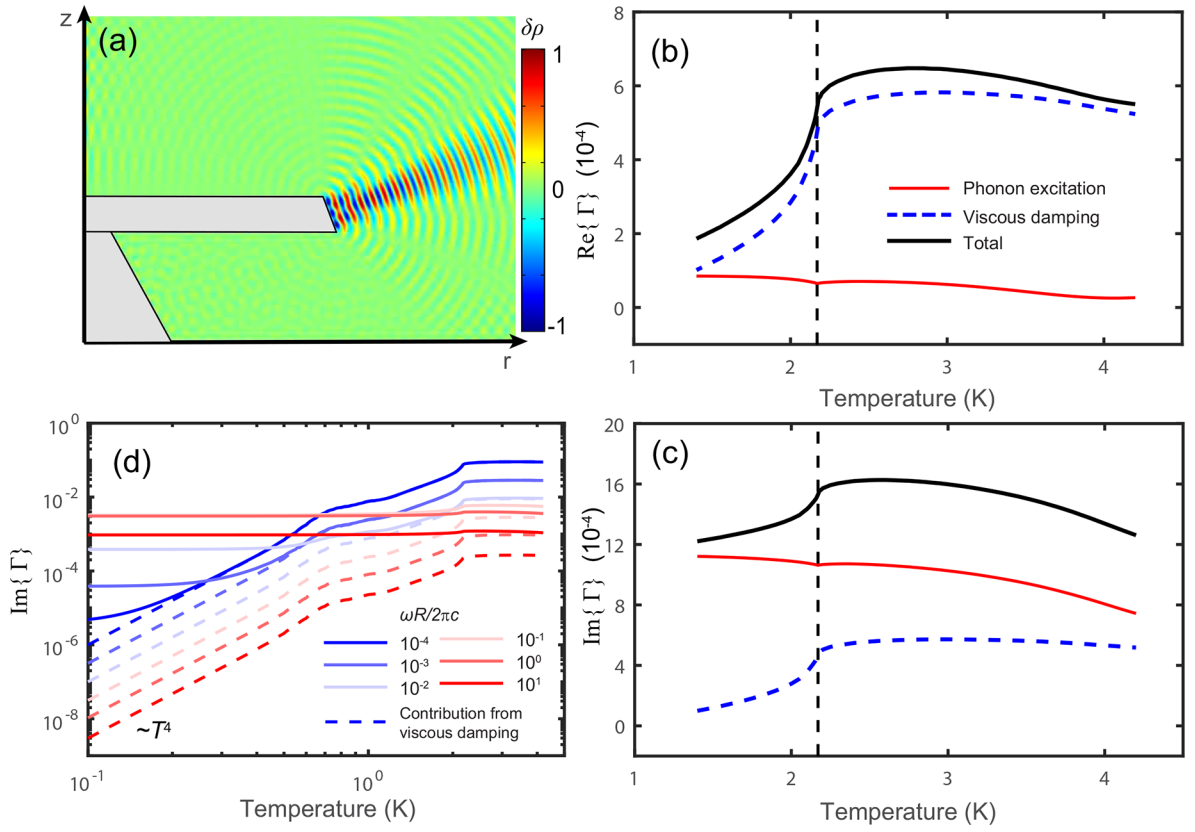

Figure 4. Predictions of the theoretical model. (a) Color-plot of the simulated liquid ^{4}He phonon wave in the vicinity of the nanomechanical resonator in cylindrical coordinates. The color scale represents the normalized density field of liquid ^{4}He. The gray region is the microdisk resonator, which has a thickness of 0.65 um and top-radius of 4.4 μm. (b) Re{Γ} and (c) Im{Γ} plotted against temperature. The black dashed line indicates the λ-point. (d) Im{Γ} plotted against temperature for various $R\omega/c$ ratios. The contribution from the shear viscous damping is plotted in dashed lines.

to the largest amplitude of A = 1.78 pm attained in the experiment. This corresponds to a peak velocity of ωA = 8.9 mm/s. The linearity of the device response ensures that nonlinear effects such as generation of cavitation, quantum turbulence, and mutual friction are negligible.

Subsequently, the temperature dependence of the quality factor and the resonance frequency were measured in LHe and are plotted in Figure 3a and 3b. In these measurements, an optical power of −17 dBm and RF power of −15 dBm were used. In general, the frequency and quality factor vary smoothly with temperature, but a clear kink in both f_m and Q_m is observed at the λ-point T = 2.17 K where the phase transition from He-I to He-II phase takes place. While the quality factor shows an increasing trend as the temperature drops below the λ-point, the rise slowly saturates resulting in a quality factor at T = 1.45 K even lower than that at T = 4.2 K. This is counterintuitive because at T = 1.45 K over 90% of the ^{4}He is in the superfluid phase which carries no viscosity, so one would naively expect that the losses should be greatly reduced. In the following, we present evidence that such loss is mainly due to coupling to the phonons in the superfluid helium (i.e., excitation of first-sound waves) which irreversibly radiate to the open environment. We also show that once the superfluid phonon is confined in a cavity, strong coupling can be achieved.

We develop a numerical method based on refs 43−45 to analyze the coupled dynamics of the superfluid and the nanomechanical resonator. Detailed discussion of the model is presented in the Supporting Information. Consider the following two coupled processes: (I) the nanomechanical resonator's oscillatory motion actuates the flow of the surrounding superfluid, and in turn, (II) the superfluid exerts force on the resonator through momentum exchange. A self-consistent solution can be obtained by combining the two coupled processes.

To analyze the actuation of the superfluid by the resonator, we applied the phenomenological Landau−Khalatnikov two-fluid model.[46] The complete set of PDEs describing the flow of mass, momentum, and entropy can be solved using an oscillatory boundary condition to account for the vibration of the nanomechanical resonator. Because of the very large kinetic Reynolds number $\mathrm{RE_k} = \rho_n \omega R^2/\eta \approx 10^6$ and large $\omega R/c \approx 10^2$ ratio, where ρ_n, η, and c are the normal fluid density, viscosity, and speed of sound of liquid ^{4}He, the flow is predominantly inviscid and the fluid compressibility, thus radiation damping, is important. We solve the problem using an inviscid model combined with a boundary layer method that accounts for the shear viscous effect. The dynamic Reynolds number $\mathrm{RE_d} = \rho_n \omega A R/\eta < 1$ remains small, and so inertial effects such as nonlaminar flow can be neglected. We solve for the PDE problem using FEM. A calculated density field of the phonon waves generated around the resonator is shown in Figure 4a.

To analyze the back-action from the superfluid to the resonator, we consider the equation of motion for a nanomechanical resonator operates inside a fluid:

DOI: 10.1021/acs.nanolett.9b00821
Nano Lett. XXXX, XXX, XXX−XXX

Table 1. Comparison of Key Device Parameters of Micro-/Nanomechanical Resonators Operated in Superfluid Helium

ref	Resonator type	T	m_e	f_m	x_{zp} [a]	$\bar{n}_{th}$ [b]	Q_m	$\frac{k_B T}{h f_m Q_m}$
This work	Microdisk	1.45 K	136 pg	817.7 MHz	0.27 fm	37	850	0.044
32	Nanobeam	1.3 K	2.4 pg	1.14 MHz	55 fm	2.4×10^4	23	1070
18,30,31	Parallel plates	60 mK	345 ng	23.1 kHz	1.03 fm	5.4×10^4	10^5	0.54
25	Vibrating wire	155 μK	2.82 μg	9.857 kHz	0.55 fm	330	1490	0.22
28	Tuning fork	1.55 K	3.05 μg	159.4 kHz	0.13 fm	2.0×10^5	3190	63
29	Tuning fork	0.35 K	173 μg	74.5 kHz	26 am	9.8×10^4	7.6×10^4	1.3
26	Grid	10 mK	0.1 g	926 Hz	9.5 am	2.2×10^5	2.5×10^5	0.9

[a] $x_{zp} = \sqrt{\hbar/4\pi m_e f_m}$ is the quantum zero-point displacement. [b] $\bar{n}_{th} = k_B T/h f_m$ is the thermal occupation.

$m_e\ddot{x} + (m_e\Omega_m/Q_i)\dot{x} + m_e\Omega_m^2 x = F_f + F_{ex}$, where Ω_m, Q_i, and m_e are the resonance frequency, intrinsic quality factor, and effective mass in absence of the fluid, and F_f and F_{ex} are the fluidic force and external driving force. A detailed analysis shows that F_f is predominately determined by the phonon dynamics in the superfluid while the effect of the temperature and entropy oscillation is negligible (see Supporting Information). The fluidic force $F_f = F_p + F_v$ can be further divided into contributions from the phonon pressure force F_p and shear viscous force F_v.

Results of the two coupled processes can be combined to obtain a self-consistent solution. In a linear regime, the fluidic force F_f is a linear response to x. One can define a dimensionless hydrodynamic function $\Gamma[\omega] = F_f[\omega]/m_e\omega^2 x[\omega]$.[16,19,43] (The definition here differs from those in refs 16 and 43 by a geometrical factor.) Its real part Re{Γ} represents the mass-loading effect that modifies the resonance frequency $\Omega_f = \Omega_m/\sqrt{1 + \mathrm{Re}\{\Gamma\}}$, and its imaginary part Im{Γ} represents the fluidic damping that modifies the quality factor $Q_f^{-1} = Q_i^{-1} + \mathrm{Im}\{\Gamma\}$.

From the measured quality factor and frequency shift (relative to that in vacuum), Re{Γ} and Im{Γ} are extracted and plotted in Figure 3c and 3d. Also shown are the computed hydrodynamic functions based on the model, which agrees very well with the experimental results. In the calculation, material parameters including viscosity and density fraction of the superfluid are the experimentally measured values from ref 47. The effective boundary length δ_e (see Supporting Information eq S42) is found to be ∼3.8 times the Stokes boundary length $\delta_B = \sqrt{\eta/\rho_n\omega}$, which is $\delta_B \approx 2$−5 nm throughout the temperature range. We attribute this increase in effective boundary length to the surface roughness of the materials, which is expected to cause additional fluid trapping at the surface and hence stronger viscous effects.[48]

To gain more physical insight, we plot the hydrodynamic functions contributed from phonon excitation Γ_p and from viscous damping Γ_v in Figure 4b and 4c. One can see that at low temperature the viscous effect is reduced significantly while the effect of phonon excitation stays strong, resulting in a higher dissipation ($\mathrm{Im}\{\Gamma\} \approx Q_m^{-1}$) at 1.45 K than at 4.2 K. At T = 1.45 K, the effect of phonon excitation accounts for over $\mathrm{Im}\{\Gamma_p\}/\mathrm{Im}\{\Gamma\}$ = 92% of the overall dissipation. For the device with R = 4.2 um, f_m = 817.7 MHz, and Q_m of 850, the average number of thermal phonons is $\bar{n}_{th} = [\exp(h f_m/k_B T) - 1]^{-1}$ = 37. The dissipation rate corresponds to an average exchange of 0.25 phonons per period of oscillation between the nanomechanical resonator and the superfluid. This sets the minimum operation level of the device as a phonon transducer. This is also equivalent to $k_B T/h f_m Q_m = 0.044$. Attaining $k_B T/h f_m Q_m \ll 1$ is a key requirement for quantum operation of nanomechanical resonators.[49,50] To our best knowledge, the value we achieved here is the lowest among all demonstrations of micro/nanomechanical resonators immersed in superfluid Helium; see Table 1 for comparison.

The efficient phonon excitation in our system can be attributed to the large $\omega R/c$ ratio, which is the dimensionless wavenumber of the flow. This is illustrated in Figure 4d, which plots Im{Γ} versus temperature for different $\omega R/c$. In this calculation, the geometry and dimensions are kept constant while ω is varied. Also shown is the viscous contribution. In all cases, the latter drops quickly at low temperature as $\sim T^4$. As $\omega R/c$ increases, the viscous effect is reduced while the phonon excitation effect rises; eventually the latter dominates the dissipation in the whole temperatures range. This behavior could provide an explanation to the saturation of resonator dissipation at low temperature observed in previous studies.[31]

The efficient phonon excitation in ^{4}He suggests that one can realize strong coupling between the nanomechanical phonons and superfluidic phonons when the latter are confined in cavities. To illustrate this, we simulate a system which consists of a microdisk and an outer ring structure that prevents the superfluid phonon from radiating away. The gap forms an open phonon cavity with cavity length L (see inset of Figure 5). Figure 5 plots the simulated mechanical response $|x[\omega]/F_{ex}[\omega]|^2$ for different L at T = 1.4 K. (Additional numerical results and analysis can be found in the Supporting Information.) For large frequency differences, the response is close to that of the uncoupled resonator (black dashed line) which has a line width of $w_{mech} = f_m/Q_m$ = 0.135 MHz. Here the quality factor is high (Q_m = 5800) mainly because of the presence of the outer ring structure that modifies the radiation of the phonon modes. When the detuning is decreased by changing L, a peak appears near the cavity phonon mode (white dashed line) with a line width of w_{cav} = 0.522 MHz. In the color plot, a clear anticrossing is visible, indicating strong coupling between the resonator and superfluidic phonon. Our simulations thus show that, even though the phonon is not confined at every side, the phonon exchange between the mechanical resonator and the superfluid is sufficiently strong to prevail the loss. From the frequency splitting 2Δ = 7.87 MHz, a single-phonon cooperativity $C = 4\Delta^2/w_{mech}w_{cav}$ = 880 is obtained.

In conclusion, in this work we experimentally demonstrate an ultrahigh-frequency nanomechanical resonator operated in superfluid ^{4}He. We show that the device dynamics is predominantly determined by the phonon coupling to superfluid (i.e., excitation of first-sound waves) rather than

DOI: 10.1021/acs.nanolett.9b00821
Nano Lett. XXXX, XXX, XXX−XXX

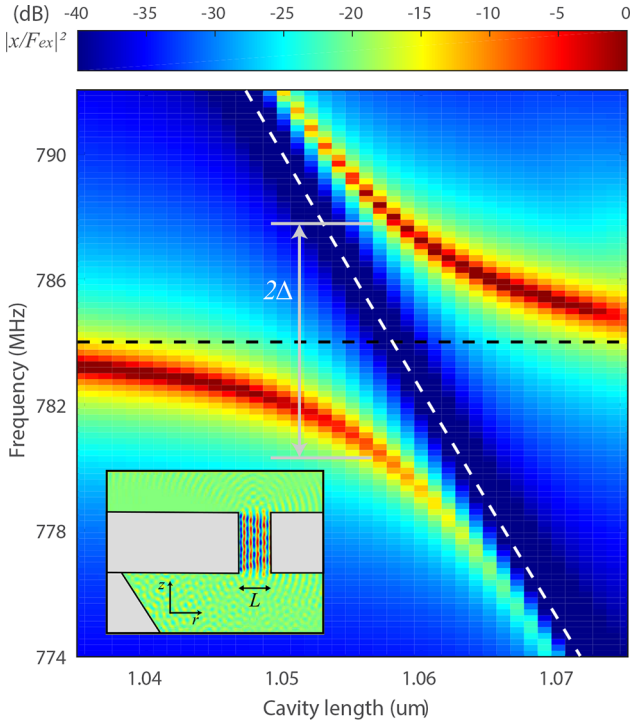

Figure 5. Strong coupling between nanomechanical resonator and superfluid phonon. Color plot shows the device response $|x[\omega]/F_{ex}[\omega]|^2$ as a function of frequency and cavity length L. The black and white dashed lines represent the uncoupled resonance frequencies of the nanomechanical resonator and the superfluid ^{4}He cavity phonon. Inset shows the simulated density field of the phonon in superfluid ^{4}He. The microdisk has a thickness of 2 μm and radius of 4.4 μm.

the viscous damping as that in many classical liquids. We further numerically show that strong coupling between the nanomechanical resonator and superfluid cavity phonons can be achieved with cooperativity up to 880. Our study opens new opportunities in control and manipulation of superfluid at the nanoscale and low-excitation level in an integrated platform. It also provides an ideal platform for studying the interaction between macroscopic quantum objects. In future work, a nonlinear regime where mutual friction between the two fluid components becomes significant can be an interesting topic for further investigation.

■ ASSOCIATED CONTENT

Supporting Information

The Supporting Information is available free of charge on the ACS Publications website at DOI: 10.1021/acs.nanolett.9b00821.

Theoretical model for the superfluid−nanostructure interaction, numerical results for strong coupling regime, values of ^{4}He dynamic viscosity used in calculations, comparison of device performance in different liquids predicted by the model, experimental setup, and additional experimental results (PDF)

■ AUTHOR INFORMATION

Corresponding Authors

*E-mail: kingyan.fong@gmail.com.
*E-mail: hong.tang@yale.edu.

ORCID

King Yan Fong: 0000-0002-8596-126X

Notes

The authors declare no competing financial interest.

■ ACKNOWLEDGMENTS

H.X.T. acknowledges support from a Packard Fellowship in Science and Engineering and a career award from the National Science Foundation. This work was funded by the DARPA/MTO ORCHID program through a grant from the Air Force Office of Scientific Research (AFOSR) and an STIR grant from Army Research Office (ARO). M.P. acknowledges support of the Technische Universität München − Institute for Advanced Study, funded by the German Excellence Initiative (and the European Union Seventh Framework Programme under Grant Agreement No. 291763). D.J.'s work is performed at the Center for Nanoscale Materials, a U.S. Department of Energy Office of Science User Facility, supported by the U.S. Department of Energy, Office of Science, under Contract No. DE-AC02-06CH11357.

■ REFERENCES

(1) Anetsberger, G.; Arcizet, O.; Unterreithmeier, Q. P.; Riviere, R.; Schliesser, A.; Weig, E. M.; Kotthaus, J. P.; Kippenberg, T. J. Near-Field Cavity Optomechanics with Nanomechanical Oscillators. *Nat. Phys.* **2009**, *5*, 909−914.

(2) Eichenfield, M.; Camacho, R.; Chan, J.; Vahala, K. J.; Painter, O. A Picogram- and Nanometre-Scale Photonic-Crystal Optomechanical Cavity. *Nature* **2009**, *459*, 550−555.

(3) Teufel, J. D.; Li, D.; Allman, M. S.; Cicak, K.; Sirois, A. J.; Whittaker, J. D.; Simmonds, R. W. Circuit Cavity Electromechanics in the Strong-Coupling Regime. *Nature* **2011**, *471*, 204−208.

(4) Cleland, A. N.; Roukes, M. L. A Nanometre-Scale Mechanical Electrometer. *Nature* **1998**, *392*, 160−162.

(5) Rugar, D.; Budakian, R.; Mamin, H. J.; Chui, B. W. Single Spin Detection by Magnetic Resonance Force Microscopy. *Nature* **2004**, *430*, 329−332.

(6) Arcizet, O.; Jacques, V.; Siria, A.; Poncharal, P.; Vincent, P.; Seidelin, S. A Single Nitrogen-Vacancy Defect Coupled to a Nanomechanical Oscillator. *Nat. Phys.* **2011**, *7*, 879−883.

(7) Kolkowitz, S.; Jayich, A. C. B.; Unterreithmeier, Q. P.; Bennett, S. D.; Rabl, P.; Harris, J. G. E.; Lukin, M. D. Coherent Sensing of a Mechanical Resonator with a Single-Spin Qubit. *Science* **2012**, *335*, 1603−1606.

(8) LaHaye, M. D.; Suh, J.; Echternach, P. M.; Schwab, K. C.; Roukes, M. L. Nanomechanical Measurements of a Superconducting Qubit. *Nature* **2009**, *459*, 960−964.

(9) O'Connell, A. D.; Hofheinz, M.; Ansmann, M.; Bialczak, R. C.; Lenander, M.; Lucero, E.; Neeley, M.; Sank, D.; Wang, H.; Weides, M.; Wenner, J.; Martinis, J. M.; Cleland, A. N. Quantum Ground State and Single-Phonon Control of a Mechanical Resonator. *Nature* **2010**, *464*, 697−703.

(10) Stannigel, K.; Rabl, P.; Sørensen, A. S.; Zoller, P.; Lukin, M. D. Optomechanical Transducers for Long-Distance Quantum Communication. *Phys. Rev. Lett.* **2010**, *105*, 220501.

(11) Kurizki, G.; Bertet, P.; Kubo, Y.; Mølmer, K.; Petrosyan, D.; Rabl, P.; Schmiedmayer, J. Quantum Technologies with Hybrid Systems. *Proc. Natl. Acad. Sci. U. S. A.* **2015**, *112*, 3866−3873.

(12) Hatanaka, D.; Mahboob, I.; Onomitsu, K.; Yamaguchi, H. Phonon Waveguides for Electromechanical Circuits. *Nat. Nanotechnol.* **2014**, *9*, 520−524.

(13) Gustafsson, M. V.; Aref, T.; Kockum, A. F.; Ekström, M. K.; Johansson, G.; Delsing, P. Propagating Phonons Coupled to an Artificial Atom. *Science* **2014**, *346*, 207−211.

DOI: 10.1021/acs.nanolett.9b00821
Nano Lett. XXXX, XXX, XXX−XXX

(14) Tadesse, S. A.; Li, M. Sub-Optical Wavelength Acoustic Wave Modulation of Integrated Photonic Resonators at Microwave Frequencies. *Nat. Commun.* **2014**, *5*, 5402.
(15) Balram, K. C.; Davanço, M. I.; Song, J. D.; Srinivasan, K. Coherent Coupling between Radiofrequency, Optical and Acoustic Waves in Piezo-Optomechanical Circuits. *Nat. Photonics* **2016**, *10*, 346−352.
(16) Paul, M. R.; Cross, M. C. Stochastic Dynamics of Nanoscale Mechanical Oscillators Immersed in a Viscous Fluid. *Phys. Rev. Lett.* **2004**, *92*, 235501.
(17) Karabacak, D. M.; Yakhot, V.; Ekinci, K. L. High-Frequency Nanofluidics: An Experimental Study Using Nanomechanical Resonators. *Phys. Rev. Lett.* **2007**, *98*, 254505.
(18) Gonzalez, M.; Zheng, P.; Garcell, E.; Lee, Y.; Chan, H. B. Comb-Drive Micro-Electro-Mechanical Systems Oscillators for Low Temperature Experiments. *Rev. Sci. Instrum.* **2013**, *84*, 025003.
(19) Fong, K. Y.; Poot, M.; Tang, H. X. Nano-Optomechanical Resonators in Microfluidics. *Nano Lett.* **2015**, *15*, 6116−6120.
(20) Burg, T. P.; Godin, M.; Knudsen, S. M.; Shen, W.; Carlson, G.; Foster, J. S.; Babcock, K.; Manalis, S. R. Weighing of Biomolecules, Single Cells and Single Nanoparticles in Fluid. *Nature* **2007**, *446*, 1066−1069.
(21) Bahl, G.; Kim, K. H.; Lee, W.; Liu, J.; Fan, X.; Carmon, T. Brillouin Cavity Optomechanics with Microfluidic Devices. *Nat. Commun.* **2013**, *4*, 1994.
(22) Han, K.; Zhu, K.; Bahl, G. Opto-Mechano-Fluidic Viscometer. *Appl. Phys. Lett.* **2014**, *105*, 014103.
(23) Gil-Santos, E.; Baker, C.; Nguyen, D. T.; Hease, W.; Gomez, C.; Lemaître, A.; Ducci, S.; Leo, G.; Favero, I. High-Frequency Nano-Optomechanical Disk Resonators in Liquids. *Nat. Nanotechnol.* **2015**, *10*, 810−816.
(24) Zhang, H.; Zhao, X.; Wang, Y.; Huang, Q.; Xia, J. Femtogram Scale High Frequency Nano-Optomechanical Resonators in Water. *Opt. Express* **2017**, *25*, 821−830.
(25) Defoort, M.; Dufresnes, S.; Ahlstrom, S. L.; Bradley, D. I.; Haley, R. P.; Guénault, A. M.; Guise, E. A.; Pickett, G. R.; Poole, M.; Woods, A. J.; Tsepelin, V.; Fisher, S. N.; Godfrin, H.; Collin, E. Probing Bogoliubov Quasiparticles in Superfluid ^{3}He with a 'Vibrating-Wire Like' MEMS Device. *J. Low Temp. Phys.* **2016**, *183*, 284−291.
(26) Efimov, V. B.; Garg, D.; Giltrow, M.; McClintock, P. V. E.; Skrbek, L.; Vinen, W. F. Experiments on a High Quality Grid Oscillating in Superfluid ^{4}He at Very Low Temperatures. *J. Low Temp. Phys.* **2010**, *158*, 462−467.
(27) Guo, W.; Jin, D.; Seidel, G. M.; Maris, H. J. Experiments with Single Electrons in Liquid Helium. *Phys. Rev. B: Condens. Matter Mater. Phys.* **2009**, *79*, 054515.
(28) Bradley, D. I.; Clovecko, M.; Fisher, S. N.; Garg, D.; Guise, E.; Haley, R. P.; Kolosov, O.; Pickett, G. R.; Tsepelin, V. Crossover from Hydrodynamic to Acoustic Drag on Quartz Tuning Forks in Normal and Superfluid. *Phys. Rev. B: Condens. Matter Mater. Phys.* **2012**, *85*, 014501.
(29) Schmoranzer, D.; La Mantia, M.; Sheshin, G.; Gritsenko, I.; Zadorozhko, A.; Rotter, M.; Skrbek, L. Acoustic Emission by Quartz Tuning Forks and Other Oscillating Structures in Cryogenic ^{4}He Fluids. *J. Low Temp. Phys.* **2011**, *163*, 317−344.
(30) Gonzalez, M.; Zheng, P.; Moon, B. H.; Garcell, E.; Lee, Y.; Chan, H. B. Unusual Behavior of a MEMS Resonator in Superfluid ^{4}He. *J. Low Temp. Phys.* **2013**, *171*, 200−206.
(31) Gonzalez, M.; Bhupathi, P.; Moon, B. H.; Zheng, P.; Ling, G.; Garcell, E.; Chan, H. B.; Lee, Y. Characterization of MEMS Devices for the Study of Superfluid Helium Films. *J. Low Temp. Phys.* **2011**, *162*, 661−668.
(32) Bradley, D. I.; George, R.; Guénault, A. M.; Haley, R. P.; Kafanov, S.; Noble, M. T.; Pashkin, Y. A.; Pickett, G. R.; Poole, M.; Prance, J. R.; Sarsby, M.; Schanen, R.; Tsepelin, V.; Wilcox, T.; Zmeev, D. E. Operating Nanobeams in a Quantum Fluid. *Sci. Rep.* **2017**, *7*, 4876.
(33) Kraus, A.; Erbe, A.; Blick, R. H. Nanomechanical Vibrating Wire Resonator for Phonon Spectroscopy in Liquid Helium. *Nanotechnology* **2000**, *11*, 165.
(34) De Lorenzo, L. A.; Schwab, K. C. Superfluid Optomechanics: Coupling of a Superfluid to a Superconducting Condensate. *New J. Phys.* **2014**, *16*, 113020.
(35) Souris, F.; Rojas, X.; Kim, P. H.; Davis, J. P. Ultralow-Dissipation Superfluid Micromechanical Resonator. *Phys. Rev. Appl.* **2017**, *7*, 044008.
(36) Harris, G. I.; McAuslan, D. L.; Sheridan, E.; Sachkou, Y.; Baker, C.; Bowen, W. P. Laser Cooling and Control of Excitations in Superfluid Helium. *Nat. Phys.* **2016**, *12*, 788−793.
(37) Kashkanova, A. D.; Shkarin, A. B.; Brown, C. D.; Flowers-Jacobs, N. E.; Childress, L.; Hoch, S. W.; Hohmann, L.; Ott, K.; Reichel, J.; Harris, J. G. E. Superfluid Brillouin Optomechanics. *Nat. Phys.* **2016**, *13*, 74−79.
(38) Fong, K. Y.; Fan, L.; Jiang, L.; Han, X.; Tang, H. X. Microwave-Assisted Coherent and Nonlinear Control in Cavity Piezo-Optomechanical Systems. *Phys. Rev. A: At., Mol., Opt. Phys.* **2014**, *90*, 051801R.
(39) Han, X.; Fong, K. Y.; Tang, H. X. A 10-GHz Film-Thickness-Mode Cavity Optomechanical Resonator. *Appl. Phys. Lett.* **2015**, *106*, 161108.
(40) Chandorkar, S. A.; Agarwal, M.; Melamud, R.; Candler, R. N.; Goodson, K. E.; Kenny, T. W. Limits of Quality Factor in Bulk-Mode Micromechanical Resonators. *Proc. IEEE MEMS.* **2008**, 74.
(41) Arcizet, O.; Rivière, R.; Schliesser, A.; Anetsberger, G.; Kippenberg, T. J. Cryogenic Properties of Optomechanical Silica Microcavities. *Phys. Rev. A: At., Mol., Opt. Phys.* **2009**, *80*, 021803R.
(42) Gorodetsky, M. L.; Schliesser, A.; Anetsberger, G.; Deleglise, S.; Kippenberg, T. J. Determination of the Vacuum Optomechanical Coupling Rate Using Frequency Noise Calibration. *Opt. Express* **2010**, *18*, 23236−23246.
(43) Sader, J. E. Frequency Response of Cantilever Beams Immersed in Viscous Fluids with Applications to the Atomic Force Microscope. *J. Appl. Phys.* **1998**, *84*, 64.
(44) Van Eysden, C. A.; Sader, J. E. Compressible Viscous Flows Generated by Oscillating Flexible Cylinders. *Phys. Fluids* **2009**, *21*, 013104.
(45) Tuck, E. O. Calculation of Unsteady Flows due to Small Motions of Cylinders in a Viscous Fluid. *J. Eng. Math.* **1969**, *3*, 29−44.
(46) Khalatnikov, I. M. *An Introduction to the Theory of Superfluidity*; W. A. Benjamin: New York, 1965.
(47) Donnelly, R. J.; Barenghi, C. F. The Observed Properties of Liquid Helium at the Saturated Vapor Pressure. *J. Phys. Chem. Ref. Data* **1998**, *27*, 1217−1274. Esel'son, B. N.; Nosovitskaya, O. S.; Pogorelov, L. A.; Sobolev, V. I. Characteristics of the Viscosity of Liquid Helium below 1K. *JETP Lett.* **1980**, *31*, 31. Dynamic viscosity at $T < 0.5$ K are obtained from extrapolation of the data using T^4 dependence (see Supporting Information).
(48) Martin, S. J.; Frye, G. C.; Ricco, A. J.; Senturia, S. D. Effect of Surface Roughness on the Response of Thickness-Shear Mode Resonators in Liquids. *Anal. Chem.* **1993**, *65*, 2910−2922.
(49) Marquardt, F.; Chen, J. P.; Clerk, A. A.; Girvin, S. M. Quantum Theory of Cavity-Assisted Sideband Cooling of Mechanical Motion. *Phys. Rev. Lett.* **2007**, *99*, 093902.
(50) Chakram, S.; Patil, Y.-S.; Chang, L.; Vengalattore, M. Dissipation in Ultrahigh Quality Factor SiN Membrane Resonators. *Phys. Rev. Lett.* **2014**, *112*, 127201.

DOI: 10.1021/acs.nanolett.9b00821
Nano Lett. XXXX, XXX, XXX−XXX